SpecBridge: Bridging Mass Spectrometry and Molecular Representations via Cross-Modal Alignment

Yinkai Wang [1] **Yan Zhou Chen** [1] **Xiaohui Chen** [1] **Li-Ping Liu** [1] **Soha Hassoun** [1 2]

Abstract

Small-molecule identification from tandem mass spectrometry (MS/MS) remains a bottleneck in untargeted settings where spectral libraries are incomplete. While deep learning offers a solution, current approaches broadly fall into two categories: explicit generative models that construct molecular graphs, or joint contrastive models that learn cross-modal subspaces from scratch. We introduce SpecBridge, a novel implicit alignment framework that treats structure identification as a geometric alignment problem from the spectra the molecular space. SpecBridge fine-tunes a self-supervised spectral encoder (DreaMS) to project directly into the latent space of a frozen molecular foundation model (ChemBERTa), and then performs retrieval by cosine similarity to a fixed bank of precomputed molecular embeddings. Across MassSpecGym, Spectraverse, and MSnLib benchmarks, SpecBridge improves top-1 retrieval accuracy by roughly 20–25% relative to strong neural baselines, while keeping the number of trainable parameters small. These results suggest that aligning to frozen foundation models is a practical, stable alternative to training new models from scratch. The code for SpecBridge is released at https://github.com/HassounLab/SpecBridge.

1. Introduction

Tandem mass spectrometry (MS/MS) is a cornerstone of untargeted metabolomics, enabling large-scale measurement of small molecules in complex biological and environmental samples. However, interpreting MS/MS spectra at scale remains a major bottleneck: despite the availability of large spectral libraries, the majority of acquired spectra cannot be confidently assigned to molecular structures (da Silva et al., 2015; Bittremieux et al., 2022). This persistent annotation gap between data generation and interpretation continues to limit downstream biological discovery.

Existing computational approaches for assigning chemical structures to a measured spectra can be broadly divided into *explicit* and *implicit* inference paradigms. Explicit methods attempt to directly model the physical or chemical processes linking molecular structure to spectra. Molecule-to-spectra approaches simulate fragmentation from putative candidate molecules that can be retrieved from large databases such as PubChem, while spectra-to-molecules approaches explicitly generate molecular structures (or fingerprints) conditioned on spectral evidence. While these approaches yield interpretable structure-level predictions, they place the primary modeling burden on explicit reconstruction, requiring the model to learn chemical fragmentation processes across various instrument settings, or to generate valid molecular structures based on spectral evidence. Hence, these approaches are sensitive to modeling assumptions, difficult to generalize across instruments, and challenging to scale due to expensive per-candidate simulation or iterative structure generation at inference time.

Implicit approaches operate at the level of learned representations, ranking candidate molecules by their similarity to a query spectrum's embedding rather than explicitly simulating spectra or constructing molecular structures. State-of-the-art methods such as JESTR, MVP, and GLMR train specialized cross-modal architectures using contrastive objectives (Kalia et al., 2025; Zhou Chen & Hassoun, 2025; Zhang et al., 2025) to learn a joint embedding space. By eschewing reconstruction tasks, these methods have demonstrated strong empirical performance on benchmark datasets. However, current methods rely on end-to-end cross-modal training using contrastive learning, therefore coupling the alignment of the molecular and spectral embedding spaces with representation learning. Importantly, current implicit approaches are mostly supervised, limiting the reuse of the rich chemical structure already captured by pretrained molecular foundation models.

To address these limitations, we propose **SpecBridge**, which introduces a novel spectra-to-molecule *implicit* mapping

[1]Department of Computer Science, Tufts University, Medford, United States [2]Department of Chemical and Biological Engineering, Tufts University, Medford, United States. Correspondence to: Yinkai Wang <yinkai.wang@tufts.edu>, Soha Hassoun <soha.hasoun@tufts.edu>.

Preprint. January 27, 2026.

paradigm. Unlike explicit construction models, SpecBridge maps spectra directly into the latent space of a fixed, pretrained molecular foundation model (ChemBERTa). Concretely, SpecBridge takes DreaMS-style spectral representations (Bushuiev et al., 2025) augmented with a lightweight projection head and aligns them to frozen ChemBERTa-style molecular representations (Chithrananda et al., 2020; Ahmad et al., 2022) using a direct alignment loss on paired spectrum–structure examples. SpecBridge offers three key advantages. First, retrieval is performed via fast nearest-neighbor search over *precomputed* molecular embeddings from a fixed, pretrained foundation model, enabling scalable and efficient ranking without explicit molecule generation or per-query encoding by a learned molecular encoder. Second, SpecBridge substantially reduces the number of trainable parameters by learning only a lightweight alignment module, providing a stable and data-efficient alternative to end-to-end cross-modal training. Third, by aligning spectra to a fixed, pretrained molecular embedding space, SpecBridge preserves the rich chemical semantics encoded in molecular foundation models, which gives rise to improved retreival performance.

We evaluate SpecBridge on three molecule retrieval benchmarks. MassSpecGym (Bushuiev et al., 2024) provides carefully designed tasks with benchmark-defined candidate sets. To assess generalization, we employ two recently introduced large datasets, Spectraverse (Gupta et al., 2025) and MSnLib (Brungs et al., 2025). We construct a controlled retrieval protocol with PubChem-derived candidate sets to mimic realistic annotation scenarios. Across these benchmarks, SpecBridge demonstrates strong gains in Recall@K, mean reciprocal rank (MRR), and structure-aware MCES metrics, while using significantly fewer trainable parameters than generative baselines. The work provides the following contributions:

- We introduce **SpecBridge**, a novel *implicit* spectra-to-molecule mapping paradigm that aligns MS/MS spectra directly to a fixed, pretrained molecular foundation model, avoiding explicit molecule construction and joint latent-space learning.
- We formulate spectra–molecule alignment as a geometry-preserving embedding alignment problem, leveraging orthogonal initialization and alignment-based training to preserve the semantic structure of the molecular embedding space while enabling stable and data-efficient learning.
- We achieve state-of-the-art performance on all benchmarks while using substantially fewer trainable parameters than end-to-end cross-modal or generative approaches. On MassSpecGym, we outperform the recent generative technique GLMR by **+16.2%** in Recall@1. Crucially, we reduce structural prediction error (MCES) by over **50%**, proving that anchoring to a rigorous chemical space enforces better structural consistency than end-to-end generation
- We provide a systematic ablation of pretraining strategies, encoder freezing schedules, and objective functions. We demonstrate that initializing the spectra encoder from self-supervised DreaMS checkpoints and optimizing a direct alignment loss to a frozen target consistently outperforms random initialization and symmetric contrastive objectives.

2. Related Work

Molecule-to-spectra annotation approaches. Molecule-to-spectra approaches simulate spectra from candidate structures and score the simulated spectra against the measured spectrum. Earlier tools such as MetFrag (Ruttkies et al., 2016) and CFM-ID (Allen et al., 2014) simulate fragmentation processes, with more recent models using GNNs to capture molecular features (Zhu et al., 2020; Young et al., 2024). The performance of these approaches depends on accurate fragmentation modeling, which is sensitive to instrument conditions and difficult to generalize across datasets. Further, by focusing on spectrum-level reconstruction rather than semantic representation learning, they offer limited support for scalable indexing or downstream integration with learned embedding spaces.

Spectra-to-molecule annotation approaches. Spectra to molecule approaches aim to deduce structure directly from spectral data. Existing methods utilize generative models to explicitly construct molecular graphs or SMILES sequences. These approaches include autoregressive models such as MSNovelist, MS-BART, and MADGEN (Stravs et al., 2022; Han et al.; Wang et al.), as well as diffusion-based approaches like DiffMS (Bohde et al., 2025). Although diffusion-based models avoid the error propagation inherent to autoregressive decoding, current spectra-to-molecule approaches remain challenged as spectral signals provide only a partial, fragmented view of the underlying molecular structure.

Contrastive spectra–molecule retrieval approaches. Recent approaches learn a shared latent space where spectra and molecules can be directly compared. This line of work evolved from unimodal spectral similarity measures, such as Spec2Vec (Huber et al., 2021a) and MS2DeepScore (Huber et al., 2021b), to full cross-modal retrieval frameworks. State-of-the-art methods like JESTR (Kalia et al., 2025) and MVP (Zhou Chen & Hassoun, 2025) train specialized encoders architectures using contrastive objectives to align spectral and molecular representations. CSU-MS^2 (Xie et al., 2025) scales contrastive learning using a large simulated corpora, while GLMR (Zhang et al., 2025) initializes

its molecular encoder from ChemFormer and jointly fine-tunes it during contrastive training, with an additional generative re-ranking stage for retrieval refinement. However, these methods typically train end-to-end and learn or re-learn chemical representations rather than leveraging fixed, pre-existing molecular foundation models.

Cross-modal alignment and foundation models. Our approach is inspired by the "foundation model alignment" pattern established in computer vision. While models like CLIP (Radford et al., 2021) train both encoders jointly, subsequent work such as Locked-image Tuning (LiT) (Zhai et al., 2022) demonstrate that freezing a strong pre-trained encoder (e.g., image) and training only the alignment adapter yields superior zero-shot performance. This strategy has been extended to audio (Elizalde et al., 2023), video (Luo et al., 2022; Fang et al., 2021), and unified sensory embeddings (Girdhar et al., 2023). Analogously, the chemical domain has recently seen the emergence of strong self-supervised foundation models for both molecular structures (Chithrananda et al., 2020) and MS/MS spectra (Bushuiev et al., 2025). However, the potential of aligning them via the LiT protocol, which locks the molecular space to enforce chemical consistency, remains unexplored in mass spectrometry.

Positioning of SpecBridge. SpecBridge introduces a novel **implicit spectra-to-molecule** annotation paradigm. Rather than explicitly constructing molecular structures or learning a joint cross-modal latent space, SpecBridge maps spectral representations directly into the continuous embedding space of a fixed, pretrained molecular foundation model. The assumption is that by adopting a LiT-style asymmetric training protocol, in which the molecular encoder (ChemBERTa) is frozen and only the spectral encoder is adapted, SpecBridge anchors spectra to a stable chemical semantic manifold. Indeed, the spectral and molecular embeddings encode compatible chemical semantics and can be aligned through a low-distortion transformation. This design distinguishes SpecBridge from existing matching approaches that jointly learn or reshape molecular representations, as well as from explicit generative methods that must solve brittle structure construction under weak spectral constraints. As a result, SpecBridge provides a stable, scalable, and chemically grounded framework for spectrum-to-structure retrieval.

3. Methodology

We introduce **SpecBridge**, a modular framework designed to bridge the semantic gap between mass spectrometry and chemical structure through geometric alignment. Unlike traditional approaches that learn cross-modal representations from scratch, SpecBridge leverages the robust, pre-learned manifolds of existing foundation models. Our approach treats the molecular embedding space as a fixed, chemically organized target and learns a precise mapping from the spectral domain to this anchor. This design reformulates structure identification from a complex generative task into a stable metric learning problem, enabling accurate and efficient retrieval.

3.1. Problem Setup and Metric Learning Formulation

Let $\mathcal{S}$ denote the high-dimensional space of tandem mass spectra and $\mathcal{M}$ the discrete space of molecular graphs. We assume access to a dataset $\mathcal{D} = \{(s_i, m_i)\}_{i=1}^{N}$ consisting of pairs of spectra $s_i \in \mathcal{S}$ and their corresponding ground-truth molecular structures $m_i \in \mathcal{M}$. Our objective is to learn a cross-modal similarity-scoring function $\mathrm{sim}(s, m)$ that accurately quantifies the compatibility between a query spectrum and a candidate molecule. In the retrieval setting, given a query spectrum s and a predefined candidates set $\mathcal{C} = \{c_1, \ldots, c_K\} \subset \mathcal{M}$, the model must rank the candidates such that the ground-truth molecule $m^* \in \mathcal{C}$ is assigned the highest score. Unlike generative approaches that model the joint distribution $P(s, m)$, we formulate this as a *metric learning* problem in a fixed embedding space: we seek to map spectral representations into a semantically organized molecular embedding space such that the cosine distance between a spectrum and its true molecule is minimized, while preserving the geometric relationships between chemically similar compounds.

3.2. Architectures

We cast the MS/MS-to-molecule identification problems as a geometry-preserving alignment problem between spectral and molecular embedding spaces. To this end, we leverage two foundation models to extract high-fidelity unimodal representations and bridge them via a lightweight, specialized mapping network.

Foundation Encoders. To capture chemical semantics, we employ a **molecular encoder** f_{mol} based on ChemBERTa-2 (Ahmad et al., 2022), a transformer model pre-trained on 77 million SMILES strings. Given a molecule m, we tokenize its SMILES representation and extract the final layer's hidden state corresponding to the `[CLS]` token: $y = f_{\text{mol}}(m) \in \mathbb{R}^{d_{\text{mol}}}$ ($d_{\text{mol}} = 768$). Crucially, we keep f_{mol} **completely frozen** during training. By freezing the molecular encoder, the target embedding space remains a stable semantic anchor that preserves the chemical knowledge acquired during large-scale pretraining and avoids catastrophic forgetting. As a result, the spectral encoding adapts to the fixed geometry of the molecular embedding space. For the **spectral encoder** f_{ms}, we initialize from a DreaMS checkpoint (Bushuiev et al., 2025), which was pre-trained on 600 million spectra to predict masked peaks. A spectrum s is processed as a sequence of peak tokens (encoding m/z and intensity) prepended with a precursor token. We ex-

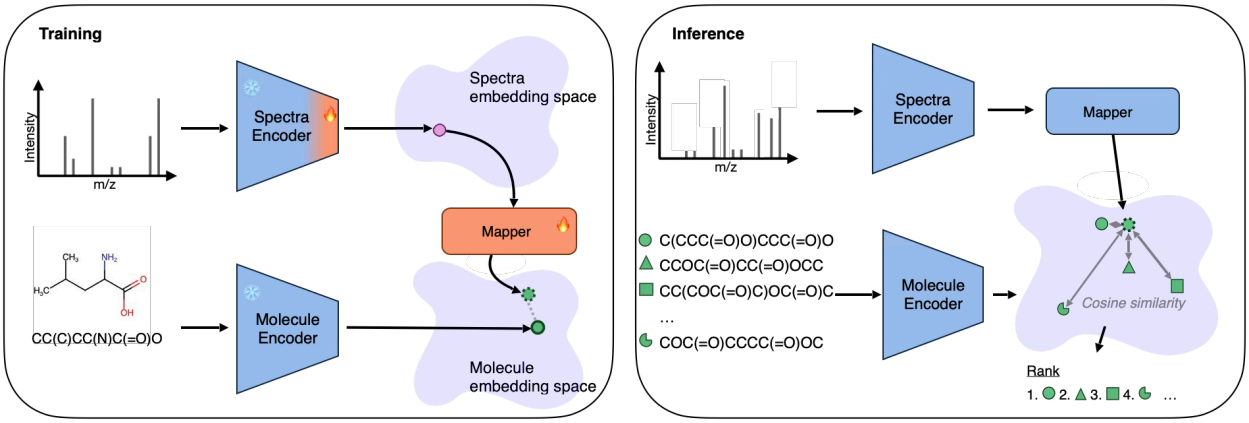

Figure 1. **The SpecBridge Framework.** We formulate structure identification as a geometric alignment problem. **(Left) Training:** The spectral encoder (top) is initialized from DreaMS and partially fine-tuned (indicated by gradient) to map inputs into the embedding space of a **frozen** ChemBERTa molecular encoder (bottom, indicated by snowflake). A lightweight **Residual Projection Mapper** aligns the spectral representation to the fixed molecular target using a direct regression objective. **(Right) Inference:** Retrieval is performed by projecting the query spectrum into the shared space and ranking pre-computed candidate embeddings via fast cosine similarity search.

tract the precursor token's final representation $x_{\text{ms}} \in \mathbb{R}^{d_{\text{ms}}}$ ($d_{\text{ms}} = 1024$) and pass it through a learnable projection head a_ϕ, a two-layer MLP with GeLU activation, to obtain a spectrum embedding $x_{proj} = a_\phi(x_{\text{ms}}) \in \mathbb{R}^{d_{\text{proj}}}$ ($d_{\text{proj}} = 2048$), which serves as an input to the alignment network. To balance plasticity and stability, we fine-tune only the projection head and the **last two transformer blocks** of f_{ms}; earlier layers, which capture fundamental physical rules of fragmentation, remain frozen.

Residual Projection Mapper. We bridge the modality gap using a mapper $g_\theta : \mathbb{R}^{d_{\text{proj}}} \to \mathbb{R}^{d_{\text{mol}}}$ designed as a geometry-preserving bridge. The architecture begins with a linear projection $W \in \mathbb{R}^{d_{\text{mol}} \times d_{\text{proj}}}$ ($d_{\text{proj}} = 2048$) that maps the spectral features to the molecular dimension ($d_{\text{mol}} = 768$). This is followed by a stack of $n = 8$ residual blocks. Formally,

$$z_0 = Wx + b$$
$$z_k = z_{k-1} + \text{MLP}_k(\text{LayerNorm}(z_{k-1})),$$

where MLP_k utilizes an *inverted bottleneck* design ($768 \to 2048 \to 768$) to facilitate feature mixing in a high-dimensional space while preserving the residual flow in the semantic manifold.

To ensure stable convergence, we initialize the linear map W using Orthogonal Initialization (Saxe et al., 2013). Specifically, since $d_{\text{mol}} < d_{\text{proj}}$, we initialize W to be row-orthogonal (semi-orthogonal) such that $WW^\top = I_{d_{\text{mol}}}$. Unlike standard Xavier or Gaussian initialization, which can alter the magnitude of activation variances, orthogonal initialization ensures that the mapper starts as a semi-orthogonal projection. This minimizes the initial distortion of the spectral embedding geometry, yielding a better-conditioned starting point for alignment than standard random initialization.

3.3. Training Objectives

Cosine Alignment and Optimization. We utilize cosine similarity as our inference metric, so we normalize all embeddings to the unit hypersphere: $\hat{y} = y/\|y\|_2$ and $\hat{z} = z/\|z\|_2$. With L2-normalized embeddings, maximizing cosine similarity between the molecular and spectral embedding is equivalent, up to a constant factor, to minimizing Euclidean distance on the unit sphere. Hence, we minimize the squared Euclidean distance between $\hat{z}$ and $\hat{y}$, using a Mean Squared Error (MSE) objective:

$$\mathcal{L}_{\text{align}} = \frac{1}{B}\sum_{i=1}^{B} \|\hat{z}_i - \hat{y}_i\|_2^2 \equiv \frac{1}{B}\sum_{i=1}^{B}(2 - 2\langle \hat{z}_i, \hat{y}_i \rangle).$$

Unlike contrastive losses (e.g., InfoNCE), which rely on a sparse signal from negative samples to push embeddings apart, this alignment objective provides a dense supervisory signal, explicitly guiding the spectral embedding to the exact coordinates of its molecular pair. This is particularly effective given that our target space is fixed and highly structured.

Geometric Regularization. To prevent the mapper from learning a degenerate mapping that collapses the embedding space (e.g., mapping all spectra to a single point), we impose a soft orthogonality constraint on the linear projection W. We minimize the Frobenius norm deviation of the Gram matrix from the identity:

$$\mathcal{L}_{\text{ortho}} = \|WW^\top - I\|_F^2.$$

The total loss is $\mathcal{L} = \mathcal{L}_{\text{align}} + \lambda_{\text{ortho}}\mathcal{L}_{\text{ortho}}$. This regularization constrains the mapping to be a **quasi-isometry**, encouraging the model to preserve the relative distances between data points. Effectively, this "rotates" and "slides" the spectral manifold onto the molecular manifold without topologically

tearing it or distorting the chemical neighborhoods established by ChemBERTa.

3.4. Inference

The SpecBridge design is optimized for high-throughput, low-latency retrieval in real-world settings. Because the molecule encoder f_{mol} is frozen, we can use **precomputed** embeddings $\mathbf{Y}_{\mathcal{C}} \in \mathbb{R}^{|\mathcal{C}| \times d_{\text{mol}}}$ for the entire candidate library (e.g., PubChem, HMDB). At inference time, for a query spectrum s, we perform a single forward pass through the spectral encoder and mapper to obtain the query vector $\hat{z}$. Ranking is then reduced to a single matrix-vector multiplication:

$$\text{Scores} = \mathbf{Y}_{\mathcal{C}} \cdot \hat{z}^{\top},$$

followed by a top-k sort. This formulation decouples the heavy molecular encoding from the query process. This allows for millisecond-scale retrieval against million-molecule databases using standard vector search libraries, a significant efficiency advantage over cross-modal attention models that require re-encoding candidates for every new query.

4. Experiments

4.1. Experimental Settings

Task Definition. We adopt the standard *molecule retrieval* task defined in MassSpecGym (Bushuiev et al., 2024). Consistent with the formulation in Section 3, this protocol mirrors real-world applications where practitioners identify unknown spectra by searching against large reference databases or running computational annotation tools.

Benchmarks and Protocols. We evaluate SpecBridge on three datasets with increasing levels of difficulty (statistics in Table 1):

- **MassSpecGym (Bushuiev et al., 2024):** We utilize the provided benchmark split and candidate pools to allow for fair comparisons with existing methods. The candidate pools are relatively small (mean size 162.5), representing a "target screening" scenario.
- **Spectraverse (Gupta et al., 2025):** To approximate a realistic open-world setting, we construct a custom retrieval protocol on the Spectraverse dataset. Since no official candidates are provided, we retrieve per-query candidate pools from **PubChem** based on the exact neutral molecular formula. This results in candidate pools that are $\approx 10\times$ larger than MassSpecGym (Avg. 1494 vs 162), presenting a significantly harder challenge that tests the model's discriminative power against isomers. We use an 8:1:1 formula-disjoint split to ensure we test generalization to unseen chemical classes rather than memorization.
- **MSnLib (Brungs et al., 2025):** We extend our evaluation to MSnLib ($\sim$560k spectra), a dataset curated under strict, standardized acquisition protocols. This benchmark allows us to validate performance on high-quality, uniform spectral data while retaining the challenging open-world PubChem candidate retrieval protocol.

Metrics. We report **Recall@K** ($K = 1, 5, 20$) and **Mean Reciprocal Rank (MRR)** to measure identification accuracy. To assess structural plausibility when the exact match is not found, we report **MCES@1** (Maximum Common Edge Subgraph distance), where lower values indicate the predicted molecule is structurally similar to the ground truth (Kretschmer et al., 2023).

Baselines. We compare SpecBridge against a comprehensive suite of methods ranging from classical baselines (DeepSets (Zaheer et al., 2017), Feed-froward networks (FFNs) based on fingerprints (Wei et al., 2019)) to state-of-the-art deep learning models: MIST (Goldman et al., 2023), JESTR (Kalia et al., 2025), MVP (Zhou Chen & Hassoun, 2025), and GLMR (Zhang et al., 2025). All methods use identical candidate pools. GLMR results are omitted for Spectraverse/MSnLib as official training implementation is not currently available.

Implementation Details. SpecBridge uses a frozen ChemBERTa encoder ($d_{\text{mol}} = 768$) and a DreaMS spectrum encoder ($d_{\text{ms}} = 1024$) adapted via a projection head ($d_{\text{proj}} = 2048$). We fine-tune only the last two transformer blocks of the spectrum encoder. The mapper uses 8 residual blocks. Optimization uses AdamW (lr=10^{-4}) with the alignment objective $\mathcal{L}_{\text{align}}$ and orthogonality penalty $\lambda_{\text{ortho}} = 10^{-3}$.

4.2. Results

SpecBridge achieves State-of-the-Art on MassSpecGym. As shown in Table 2, SpecBridge achieves a decisive improvement over all prior methods. It surpasses the strongest baseline, GLMR, by **+16.2%** in Recall@1 (68.5% $\rightarrow$ 84.7%). This performance leap is particularly notable because GLMR utilizes a complex generative diffusion process, whereas SpecBridge relies on a simple cosine similarity. Furthermore, MCES@1 is more than halved (5.05 $\rightarrow$ 2.37). A reduction of this magnitude in MCES implies that when SpecBridge fails to identify the exact molecule, the predicted candidate shares a significantly larger common subgraph with the ground truth, often differing only by minor functional group modifications rather than an incorrect scaffold. This validates our hypothesis that aligning to a continuous, pre-structured molecular space preserves chemical semantics better than generating discrete graphs or fingerprints.

Scaling to Spectraverse and MSnLib. On Spectraverse, where candidate pools are $10\times$ larger and derived from

Dataset	#Spectra	#Molecules	#Formulas	Split rule	Cand. source	Cand. size (test mean)
MassSpecGym	227,495	31,448	17,547	Benchmark	Provided	162.5
Spectraverse	464,346	42,308	22,735	Formula-disjoint	PubChem	1494.0
MSnLib	560,084	48,597	21,107	Formula-disjoint	PubChem	3041.1

Table 1. **Dataset statistics and evaluation protocol summary.** Candidate-set size is reported as the *mean per-query pool size on the test split*. For Spectraverse, candidate pools are retrieved from PubChem by exact neutral formula and are used only at inference time.

MassSpecGym					
Method	Recall@1	Recall@5	Recall@20	MRR	MCES@1 ↓
Random	2.470	10.584	21.251	5.411	13.51
DeepSets	4.699	12.355	29.289	9.901	13.12
Fingerprint FFN	4.978	15.505	33.168	11.193	13.09
DeepSets + Fourier	10.104	22.015	40.681	16.967	13.01
MIST	10.942	23.815	44.634	18.257	12.75
JESTR	11.772	33.258	61.006	22.825	11.73
MVP	13.961	36.882	68.119	26.261	10.365
GLMR	68.478	78.087	84.216	72.472	5.05
SpecBridge (Ours)	**84.695**	**92.310**	**96.850**	**88.149**	**2.37**
Spectraverse					
Method	Recall@1	Recall@5	Recall@20	MRR	MCES@1 ↓
Random	1.319	6.231	18.982	4.913	11.94
DeepSets	1.620	9.084	24.632	6.362	12.33
Fingerprint FFN	4.889	15.674	34.327	11.138	10.82
DeepSets + Fourier	6.800	21.805	40.805	14.573	9.520
MIST	7.827	31.508	53.755	19.610	7.306
JESTR	5.688	17.782	39.022	10.173	12.725
MVP	1.194	7.175	23.202	5.280	13.686
GLMR	–	–	–	–	–
SpecBridge (Ours)	**36.580**	**46.357**	**58.922**	**41.766**	**6.76**
MSnLib					
Method	Recall@1	Recall@5	Recall@20	MRR	MCES@1 ↓
Random	0.649	3.115	8.622	3.115	14.11
DeepSets	0.817	5.092	13.523	3.562	13.57
Fingerprint FFN	1.955	7.965	18.049	5.525	12.91
DeepSets + Fourier	4.031	13.479	27.627	9.28	11.61
MIST	16.270	35.614	53.164	25.563	8.71
JESTR	2.810	9.409	21.342	6.864	13.35
MVP	2.477	7.154	17.003	4.581	12.98
GLMR	–	–	–	–	–
SpecBridge (Ours)	**53.368**	**59.874**	**67.087**	**56.875**	**6.14**

Table 2. **Main retrieval results across three benchmarks.** We report Recall@K and MRR (higher is better) and the structure-aware MCES@1 metric (lower is better). Missing entries (–) indicate methods where official training implementations were unavailable. Best results in each column are marked in **bold**.

PubChem, the task is substantially harder. SpecBridge nevertheless achieves a Recall@1 of 36.6%, significantly outperforming other baselines. The decrease in performance on Spectraverse compared to MassSpecGym can be attributed to the "distractor" problem: with 1500 candidates, many candidates may have similar fragmentation patterns. SpecBridge's use of a frozen, high-fidelity molecular space allows it to maintain discriminative power even in this dense candidate regime. Similarly, on the massive MSnLib dataset (560k spectra), SpecBridge attains 53.4% Recall@1. Notably, because SpecBridge relies on cosine similarity retrieval against precomputed embeddings, it efficiently scales to these larger datasets. Inference is reduced to a fast nearest-neighbor search, avoiding the computational overhead of cross-modal attention models which typically require expensive pairwise re-encoding for every candidate in the pool.

4.3. Ablation Study

A key question is whether SpecBridge's performance stems from the proposed alignment methodology or simply from the use of strong foundation models (DreaMS/ChemBERTa). To control for this, we implemented a strong baseline using the **exact same DreaMS backbone** and fine-tuning schedule but trained with a symmetric **Contrastive loss** (details in Section A.4) instead of our direct Alignment loss.

As shown in Table 3 (Row 1 vs. Row 4), when the backbone and adaptation strategy are held constant, the Alignment objective significantly outperforms the Contrastive objective (**36.6% vs 30.4% Recall@1**). This significant gap isolates the benefit of the SpecBridge methodology: specifically, that regressing to fixed, dense molecular targets provides a superior supervisory signal than sparse negative sampling in this high-dimensional setting. Thus, while DreaMS provides a necessary geometric foundation, the choice of explicit alignment over contrastive learning is critical for maximizing retrieval performance.

4.4. Candidate pool size sensitivity

The difficulty of retrieval is largely defined by the candidate pool size. As shown in Figure 2, increasing the pool size from 128 to "all" (avg. 1494) causes a monotonic decrease in metrics, as expected. However, SpecBridge maintains robust performance even with large pools, suggesting it learns a discriminative ranking function rather than just exploiting small-pool statistics. The performance drop on Spectraverse relative to MassSpecGym is largely explained by this difference in pool size (162 vs $\approx$ 1500). The gap suggests that while SpecBridge is highly effective, the problem of distinguishing between hundreds of isomers with identical formulas but slightly modified molecular arrangements remains a fundamental challenge in mass spectrometry.

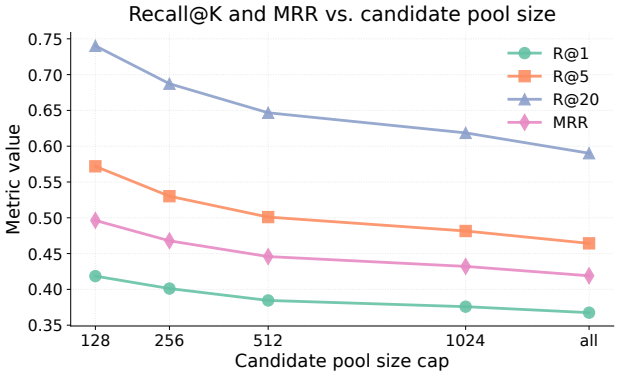

Figure 2. **Sensitivity to candidate pool size on Spectraverse.** SpecBridge performance when limiting each per-query candidate pool to at most N candidates ($N \in \{128, 256, 512, 1024\}$) versus using the full PubChem-derived pool (*all*). We report Recall@1/5/20 (top) and MRR (bottom). Larger pools increase retrieval difficulty and reduce both recall and MRR.

4.5. Training stability

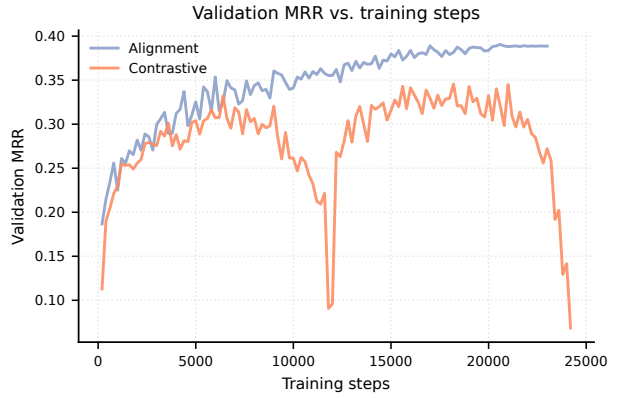

Figure 3. **Validation MRR vs. Training Steps.** We compare training stability under **strictly matched settings**: both methods employ the exact same frozen ChemBERTa molecular encoder and fine-tuned DreaMS spectral encoder. The Alignment objective (Blue) demonstrates smooth, monotonic convergence, whereas the Contrastive objective (Orange) exhibits significant volatility despite using the same fixed target space.

Training dynamics offer further evidence for the superiority of direct alignment when mapping to a foundation model. Figure 3 tracks validation performance for both objectives under identical constraints (frozen ChemBERTa target). The Alignment objective converges smoothly and reaches a higher plateau. In contrast, the Contrastive objective suffers from significant instability, characterized by sudden performance drops. We attribute this to the difficulty of optimizing an InfoNCE loss when the target space is sparse and fixed; the model struggles to maintain effective negative gradients, occasionally drifting into degenerate solutions. Conversely, direct alignment enforces stability by anchoring spectral predictions to the precise, dense coordinates of the molecular foundation space.

Configuration			Retrieval Accuracy				Structure
Objective	**Pretraining**	**Spec. Encoder**	**R@1**	**R@5**	**R@20**	**MRR**	**MCES@1 ↓**
Align	Pretrained	Fine-tune (Last-2)	**36.58**	**46.36**	**58.92**	**41.77**	**6.76**
Align	Pretrained	Frozen	31.33	41.18	54.06	36.59	7.64
Align	Random Init	Joint Train	24.34	31.99	41.89	28.73	10.15
Contrastive	Pretrained	Fine-tune (Last-2)	30.35	41.30	56.49	36.40	7.29
Contrastive	Pretrained	Frozen	27.19	36.43	50.32	32.42	7.99
Contrastive	Random Init	Joint Train	30.80	34.46	45.63	33.62	8.58

Table 3. **Ablation of design choices on Spectraverse.** We compare the performance of different training objectives (Align vs. Contrastive), initialization strategies (Pretrained vs. Random), and spectrum encoder fine-tuning schedules. The proposed **SpecBridge** configuration is highlighted in gray. Best results in each column are marked in **bold**.

4.6. Cosine-similarity separation and retrieval margin

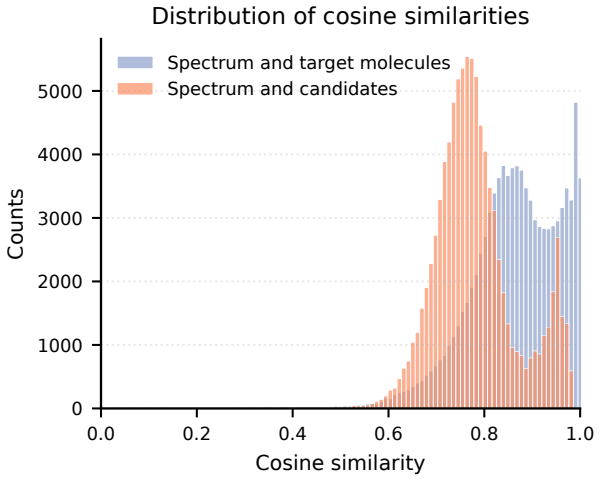

Figure 4. **Cosine-similarity separation.** Histogram of cosine similarities between each query spectrum embedding and its ground-truth molecule (blue) versus non-target candidate molecules (orange) from the retrieval pool.

Finally, we investigate the geometry of the learned space. Figure 4 demonstrates that SpecBridge successfully pulls the embeddings of spectra and their ground-truth molecules together (blue distribution, shifted right) while pushing non-target candidates away (orange distribution). The existence of this margin confirms that the mapper g_θ has successfully learned to translate spectral features into the metric space of ChemBERTa. The overlap between distributions highlights the inherent ambiguity of MS/MS: some candidates are chemically so similar to the ground truth that their spectral representations are nearly indistinguishable, setting an upper bound on retrieval accuracy.

4.7. Discussion

Our results highlight two critical design principles for scientific foundation models. First, **alignment outweighs contrastive learning** when a strong target exists. As shown in Table 3, direct regression (MSE) consistently outperforms contrastive losses. We attribute this to the nature of the supervisory signal: while contrastive learning relies on noisy, relative comparisons against batch negatives, regression to a fixed molecular anchor provides a dense, absolute error signal for every sample. Second, **freezing prevents semantic drift**. End-to-end training often allows the molecular encoder to overfit to spectral idiosyncrasies. By locking ChemBERTa, SpecBridge forces the spectral encoder to conform to a rigorous, pre-validated chemical manifold, explaining the dramatic reduction in structural errors (MCES@1) compared to baselines like GLMR.

5. Conclusion

We presented **SpecBridge**, a framework that reformulates mass spectral identification as a geometric alignment problem. By bridging a fine-tuned DreaMS encoder to a frozen ChemBERTa space via a residual projection mapper, SpecBridge achieves state-of-the-art retrieval accuracy on MassSpecGym (+16.2% Recall@1) and demonstrates robust scalability to the million-scale candidate pools of Spectraverse and MSnLib. Our findings challenge the dominance of contrastive learning in multi-modal tasks, suggesting that when robust foundation models exist, simple geometric alignment is more stable, data-efficient, and structurally accurate.

Limitations and Future Work. Performance remains bounded by the candidate library; unlike generative models, SpecBridge cannot propose novel structures outside the retrieval pool. Additionally, our alignment relies on 2D molecular graphs, ignoring the 3D conformer information inherent in mass spectra. Future work will focus on **zero-shot library expansion** to annotate spectral archives against billions of virtual molecules, and **generative decoding**, where we train a conditional generator to invert the SpecBridge embedding for *de novo* structure elucidation.

Acknowledge

Research reported in this publication was supported by the National Institute of General Medical Sciences of the National Institutes of Health under award number R35GM148219. The content is solely the responsibility of the authors and does not necessarily represent the official views of the NIH.

References

Ahmad, W., Simon, E., Chithrananda, S., Grand, G., and Ramsundar, B. Chemberta-2: Towards chemical foundation models, 2022. URL https://arxiv.org/abs/2209.01712.

Allen, F., Pon, A., Wilson, M., Greiner, R., and Wishart, D. S. CFM-ID: a web server for annotation, spectrum prediction and metabolite identification from tandem mass spectra. *Nucleic Acids Research*, 42(W1):W94–W99, 2014.

Bittremieux, W., Wang, M., and Dorrestein, P. C. The critical role that spectral libraries play in capturing the metabolomics community knowledge. *Metabolomics*, 18 (12):94, 2022.

Bohde, M., Manjrekar, M., Wang, R., Ji, S., and Coley, C. W. Diffms: Diffusion generation of molecules conditioned on mass spectra. *arXiv preprint arXiv:2502.09571*, 2025.

Brungs, C., Schmid, R., Heuckeroth, S., Mazumdar, A., Drexler, M., Šácha, P., Dorrestein, P. C., Petras, D., Nothias, L.-F., Veverka, V., et al. Msnlib: efficient generation of open multi-stage fragmentation mass spectral libraries. *Nature Methods*, pp. 1–4, 2025.

Bushuiev, R., Bushuiev, A., de Jonge, N., Young, A., Kretschmer, F., Samusevich, R., Heirman, J., Wang, F., Zhang, L., Dührkop, K., et al. Massspecgym: A benchmark for the discovery and identification of molecules. *Advances in Neural Information Processing Systems*, 37: 110010–110027, 2024.

Bushuiev, R., Bushuiev, A., Samusevich, R., Brungs, C., Sivic, J., and Pluskal, T. Self-supervised learning of molecular representations from millions of tandem mass spectra using dreams. *Nature Biotechnology*, May 2025. ISSN 1546-1696. doi: 10.1038/s41587-025-02663-3. URL https://doi.org/10.1038/s41587-025-02663-3.

Chithrananda, S., Grand, G., and Ramsundar, B. Chemberta: Large-scale self-supervised pretraining for molecular property prediction, 2020. URL https://arxiv.org/abs/2010.09885.

da Silva, R. R., Dorrestein, P. C., and Quinn, R. A. Illuminating the dark matter in metabolomics. *Proceedings of the National Academy of Sciences*, 112(41):12549–12550, 2015.

Elizalde, B., Deshmukh, S., Al Ismail, M., and Wang, H. Clap learning audio concepts from natural language supervision. In *ICASSP 2023-2023 IEEE International Conference on Acoustics, Speech and Signal Processing (ICASSP)*, pp. 1–5. IEEE, 2023.

Fang, H., Xiong, P., Xu, L., and Chen, Y. Clip2video: Mastering video-text retrieval via image clip. *arXiv preprint arXiv:2106.11097*, 2021.

Girdhar, R., El-Nouby, A., Liu, Z., Singh, M., Alwala, K. V., Joulin, A., and Misra, I. Imagebind: One embedding space to bind them all. In *Proceedings of the IEEE/CVF conference on computer vision and pattern recognition*, pp. 15180–15190, 2023.

Goldman, S., Xin, J., Provenzano, J., and Coley, C. W. Mist-cf: chemical formula inference from tandem mass spectra. *Journal of Chemical Information and Modeling*, 64(7): 2421–2431, 2023.

Gupta, V., Qiang, H., Chung, H.-H., Herbst, E., and Skinnider, M. Comprehensive curation and harmonization of small molecule ms/ms libraries in spectraverse. 2025.

Han, Y., Wang, P., Yu, K., Chen, L., et al. Ms-bart: Unified modeling of mass spectra and molecules for structure elucidation. In *The Thirty-ninth Annual Conference on Neural Information Processing Systems*.

Huber, F., Ridder, L., Verhoeven, S., Spaaks, J. H., Diblen, F., Rogers, S., and Van Der Hooft, J. J. Spec2vec: Improved mass spectral similarity scoring through learning of structural relationships. *PLoS computational biology*, 17(2):e1008724, 2021a.

Huber, F., van der Burg, S., van der Hooft, J. J., and Ridder, L. Ms2deepscore: a novel deep learning similarity measure to compare tandem mass spectra. *Journal of cheminformatics*, 13(1):84, 2021b.

Kalia, A., Zhou Chen, Y., Krishnan, D., and Hassoun, S. Jestr: Joint embedding space technique for ranking candidate molecules for the annotation of untargeted metabolomics data. *Bioinformatics*, pp. btaf354, 2025.

Kretschmer, F., Seipp, J., Ludwig, M., Klau, G. W., and Böcker, S. Small molecule machine learning: All models are wrong, some may not even be useful. *bioRxiv*, pp. 2023–03, 2023.

Langley, P. Crafting papers on machine learning. In Langley, P. (ed.), *Proceedings of the 17th International Conference on Machine Learning (ICML 2000)*, pp. 1207–1216, Stanford, CA, 2000. Morgan Kaufmann.

Luo, H., Ji, L., Zhong, M., Chen, Y., Lei, W., Duan, N., and Li, T. Clip4clip: An empirical study of clip for end to end video clip retrieval and captioning. *Neurocomputing*, 508:293–304, 2022.

Radford, A., Kim, J. W., Hallacy, C., Ramesh, A., Goh, G., Agarwal, S., Sastry, G., Askell, A., Mishkin, P., Clark, J., et al. Learning transferable visual models from natural language supervision. In *International conference on machine learning*, pp. 8748–8763. PmLR, 2021.

Ruttkies, C., Schymanski, E. L., Wolf, S., Hollender, J., and Neumann, S. Metfrag relaunch: incorporating strategies beyond in silico fragmentation. *Journal of Cheminformatics*, 8(1):3, 2016.

Saxe, A. M., McClelland, J. L., and Ganguli, S. Exact solutions to the nonlinear dynamics of learning in deep linear neural networks. *arXiv preprint arXiv:1312.6120*, 2013.

Stravs, M. A., Dührkop, K., Böcker, S., and Zamboni, N. Msnovelist: de novo structure generation from mass spectra. *Nature Methods*, 19(7):865–870, 2022.

Wang, Y., Chen, X., Liu, L., and Hassoun, S. Madgen: Mass-spec attends to de novo molecular generation. In *The Thirteenth International Conference on Learning Representations*.

Wei, J. N., Belanger, D., Adams, R. P., and Sculley, D. Rapid prediction of electron–ionization mass spectrometry using neural networks. *ACS central science*, 5(4): 700–708, 2019.

Xie, T., Zhang, H., Yang, Q., Sun, J., Wang, Y., Long, J., Zhang, Z., and Lu, H. Csu-ms2: A contrastive learning framework for cross-modal compound identification from ms/ms spectra to molecular structures. *Analytical Chemistry*, 2025.

Young, A., Wang, F., Wishart, D., Wang, B., Röst, H., and Greiner, R. Fragnnet: a deep probabilistic model for mass spectrum prediction. *arXiv preprint arXiv:2404.02360*, 2024.

Zaheer, M., Kottur, S., Ravanbakhsh, S., Poczos, B., Salakhutdinov, R. R., and Smola, A. J. Deep sets. *Advances in neural information processing systems*, 30, 2017.

Zhai, X., Wang, X., Mustafa, B., Steiner, A., Keysers, D., Kolesnikov, A., and Beyer, L. Lit: Zero-shot transfer with locked-image text tuning. In *Proceedings of the IEEE/CVF conference on computer vision and pattern recognition*, pp. 18123–18133, 2022.

Zhang, Y., Ding, K., Wu, Y., Zhuang, X., Yang, Y., Zhang, Q., and Chen, H. Breaking the modality barrier: Generative modeling for accurate molecule retrieval from mass spectra. *arXiv preprint arXiv:2511.06259*, 2025.

Zhou Chen, Y. and Hassoun, S. Learning from all views: A multiview contrastive framework for metabolite annotation. *bioRxiv*, pp. 2025–11, 2025.

Zhu, H., Liu, L., and Hassoun, S. Using graph neural networks for mass spectrometry prediction. *arXiv preprint arXiv:2010.04661*, 2020.

A. Appendix

A.1. Spectraverse candidate construction

For Spectraverse we construct per-query candidate pools that are shared across all models and remain fixed for the entirety of our experiments. Candidate pools are used *only at inference time* for validation/test evaluation.

Inputs and split. We start from a combined Spectraverse MGF file containing MS/MS spectra with metadata fields including SMILES and FORMULA. We split the dataset in an 8:1:1 ratio *by molecular formula* to prevent leakage across folds: formulas (and the associated spectra and molecules) do not appear in more than one split.

PubChem-only candidates by formula. For each validation/test query, we normalize the annotated molecular formula to PubChem's neutral convention by stripping charge-like suffixes (e.g., +2, -1, or bare +/-). We then retrieve all PubChem compounds matching the normalized formula using precomputed PubChem resources, with a rate-limited PUG-REST fallback when local resources yield no candidates. We collect candidate canonical SMILES (and InChIKeys when available), discard malformed entries, remove duplicates, and remove the query molecule itself to avoid trivial self-matches. We do not impose an artificial cap on candidate list size.

Diagnostics. The candidate construction script reports summary statistics including candidate set size distribution, the fraction of queries with zero/one/multiple candidates, and the fraction of queries requiring the PubChem API fallback.

A.2. Implementation details and hyperparameters

Trainable components. SpecBridge keeps the molecule encoder fixed (ChemBERTa) and trains: (i) a lightweight spectrum to molecule mapper g_θ (linear Procrustes-initialized map plus n residual blocks), and (ii) a small suffix of the spectrum encoder f_{ms} by unfreezing only its last two transformer blocks (all earlier layers are frozen). We also use a lightweight projection head on top of the DreaMS backbone to produce a conditioning embedding of dimension d_{cond}.

Removed DreaMS heads. We discard task-specific heads from the released self-supervised DreaMS checkpoint (e.g., peak masking and retention-order heads) and retain only the transformer backbone for encoding spectra.

Optimization. Unless stated otherwise, we train using AdamW with learning rate 10^{-4}, batch size 128, and 2 epochs. We save checkpoints every 200 steps and select the final model by validation Recall@5. We use an alignment-dominated objective with a small orthogonality penalty on the linear map.

Setting	Value
Spectrum encoder init.	DreaMS self-supervised checkpoint
Molecule encoder init.	ChemBERTa (`Derify/ChemBERTa_augmented_pubchem_13m`)
Trainable spectrum layers	last-2 transformer blocks (others frozen)
Mapper	Orthogonal linear map + $n = 8$ residual blocks
Mapper hidden width	2048
Conditioning dim d_{cond}	2048
Learning rate	1×10^{-4}
Batch size	128
Epochs	2
Checkpointing	every 200 steps
Model selection	validation Recall@5
Orthogonality weight λ_{ortho}	10^{-3}
Alignment weight w_{map}	5.0
Contrastive weights	$w_{\text{con}} = 1.0$, $w_{\text{con\_mapped}} = 1.0$ (defaults; standard alignment runs use $w_{\text{con}} = 0$, $w_{\text{con\_mapped}} = 0$)
Temperature (contrastive)	0.07

Table 4. **Default hyperparameters for SpecBridge.** Values shown correspond to our standard training configuration; we report any deviations in the experiment description. All values are confirmed from the training code and standard run configurations.

A.3. Trainable parameter breakdown

We report the number of trainable parameters in each component to quantify the degree of adaptation. Let P_{mol} denote the molecule encoder parameters, P_{ms} the spectrum encoder parameters, and P_{map} the mapper parameters. In SpecBridge, P_{mol} is fully frozen; we train P_{map} and only a small suffix of P_{ms}.

Component	#Params	#Trainable
Molecule encoder (ChemBERTa)	43,961,088	0
Spectrum encoder (DreaMS total)	95,549,381	25,174,016
Spectrum projection head	6,299,648	6,299,648
Mapper g_θ	26,774,272	26,774,272
Total	172,584,389	58,247,936

Table 5. **Trainable parameter counts.** SpecBridge updates only the mapper and a small suffix of the spectrum encoder (last two transformer blocks), while keeping ChemBERTa fixed. Parameter counts are confirmed by loading the actual models in the training environment.

A.4. Contrastive Baseline Implementation Details

To rigorously evaluate the efficacy of our direct alignment objective, we compared SpecBridge against a strong contrastive baseline trained under identical architectural constraints. The baseline employs the InfoNCE loss to maximize the mutual information between paired spectra and molecules.

Loss Formulation. We utilize a symmetric implementation of InfoNCE with a learnable temperature parameter. Given a batch of N pairs, let $z_s \in \mathbb{R}^{N\times d}$ and $z_m \in \mathbb{R}^{N\times d}$ denote the batch of spectral and molecular embeddings, respectively. The embeddings are first normalized to the unit hypersphere: $\hat{z} = z/\|z\|_2$.

We compute the similarity logits scaled by a temperature τ:

$$\text{Logits}_{ij} = \frac{\hat{z}_{s,i} \cdot \hat{z}_{m,j}^{\top}}{\tau},$$

where τ is a learnable parameter initialized to 0.07 and clamped to a minimum of 10^{-6} for numerical stability.

The total loss is the average of the spectrum-to-molecule and molecule-to-spectrum cross-entropy losses:

$$\mathcal{L} = \frac{1}{2}\left(\mathcal{L}_{s\to m} + \mathcal{L}_{m\to s}\right),$$

where $\mathcal{L}_{s\to m}$ represents the cross-entropy loss computed along the rows (identifying the correct molecule for each spectrum among in-batch negatives), and $\mathcal{L}_{m\to s}$ is computed along the columns.

Controlled Comparison Settings. Crucially, to isolate the impact of the loss function, this baseline adhered to the exact same "locked" constraints as SpecBridge:

- **Frozen Target Space:** The molecular encoder f_{mol} (ChemBERTa) was kept completely frozen. The contrastive loss updated only the spectral encoder to align with the fixed molecular anchors.
- **Architecture:** The spectral encoder used the exact same fine-tuning schedule (frozen backbone + fine-tuned last 2 layers) and projection dimension ($d_{\text{proj}} = 2048$) as the SpecBridge alignment model.

This setup ensures that the performance gap observed in Table 3 is attributable solely to the supervisory signal (Contrastive vs. Alignment) rather than architectural differences.

A.5. Additional ablations

This section collects additional ablations that can be included to further validate design choices.

Mapper capacity. We recommend varying mapper depth $n \in \{0, 2, 4, 8\}$ (with n=0 being linear-only) and hidden width $h \in \{512, 1024, 2048\}$, holding all other settings fixed, to verify that performance is not narrowly tied to a single capacity choice. As shown in Table 6, we observe that retrieval accuracy consistently improves as model capacity increases. Linear mappers ($n = 0$) lag significantly behind non-linear variants, confirming the necessity of deep projection. While performance gains saturate slightly between $n = 2$ and $n = 4$, the largest configuration ($n = 8, h = 2048$) yields the best overall results (R@1 36.6%, MRR 41.8), suggesting that the high-dimensional spectral feature space benefits from increased expressivity in the projection head.

Table 6. **Mapper Capacity Ablation.** Impact of varying residual depth (n) and hidden width (h) on performance. The proposed **SpecBridge** configuration is highlighted in gray.

Mapper Config		Retrieval Accuracy				Structure
Depth (n)	**Width** (h)	**R@1**	**R@5**	**R@20**	**MRR**	**MCES@1** ↓
0	512	26.209	35.402	48.979	31.430	8.40
0	1024	27.026	36.366	49.973	32.296	8.26
0	2048	27.646	37.048	50.625	32.907	8.13
2	512	29.687	39.154	52.079	34.908	7.95
2	1024	30.492	39.916	52.900	35.715	7.77
2	2048	31.155	41.112	53.931	36.513	7.64
4	512	29.693	39.318	52.401	34.979	7.88
4	1024	30.557	40.016	53.205	35.791	7.75
4	2048	31.171	41.067	54.076	36.505	7.64
8	512	29.825	39.615	52.668	35.135	7.87
8	1024	30.629	40.170	53.489	35.838	7.75
8	2048	**36.580**	**46.357**	**58.922**	**41.766**	**6.76**

Spectrum unfreezing depth. We evaluated unfreezing schedules (frozen; last-1; last-2; last-4 blocks) to quantify the effect of limited spectrum-side adaptation on retrieval. Table 7 demonstrates that fine-tuning the spectrum encoder is critical for aligning the modalities, with any unfreezing strategy significantly outperforming the frozen baseline. Performance peaks when unfreezing the last 2 blocks (R@1 36.58%, MRR 41.77). Interestingly, unfreezing deeper into the network (last-4 blocks) degrades performance compared to the last-2 setting, suggesting that the lower layers of the pre-trained encoder capture robust features that should be preserved, or that more aggressive fine-tuning leads to overfitting on the target dataset.

Table 7. **Spectrum Encoder Adaptation.** Impact of unfreezing different numbers of transformer blocks. The proposed **SpecBridge** configuration is highlighted in gray.

	Retrieval Accuracy				Structure
Unfreezing Scope	**R@1**	**R@5**	**R@20**	**MRR**	**MCES@1** ↓
Frozen (0)	31.327	41.179	54.061	36.587	7.64
Last-1 (1)	36.186	46.084	58.931	41.494	6.81
Last-2 (2)	**36.580**	**46.357**	**58.922**	**41.766**	**6.76**
Last-4 (4)	33.612	42.588	55.099	38.548	7.23

Impact of Orthogonal Initialization. A key component of SpecBridge is initializing the linear mapper W using Orthogonal Initialization (Saxe et al., 2013), rather than standard random (e.g., Xavier) initialization. Table 8 quantifies the benefit of this geometric stability. Using Orthogonal initialization yields a **+2.3% absolute gain** in Recall@1 (36.58% vs 34.24%) and improves MRR by over 2 points compared to a standard random initialization. This confirms that starting the mapper as an approximate isometry, which preserving the internal distances of the spectral embedding space before optimization begins, provides a superior condition for alignment than allowing random initial distortions.

A.6. Compute Resources and Efficiency

All experiments were conducted on a single NVIDIA A100 (80GB) GPU.

Table 8. **Effect of Mapper Initialization.** Comparison of performance when initializing the linear projection W via Orthogonal Initialization versus standard random (Xavier) initialization. All other hyperparameters are identical. The proposed **SpecBridge** configuration is highlighted in gray.

	Retrieval Accuracy (%)				Structure
Initialization	**R@1**	**R@5**	**R@20**	**MRR**	**MCES@1** ↓
Random (Xavier)	34.24	44.31	56.68	39.55	7.11
Orthogonal	**36.58**	**46.36**	**58.92**	**41.77**	**6.76**

Training. Training SpecBridge on MassSpecGym takes approximately **1 hours 20 minutes** for 2 epochs. This is significantly faster than GLMR (reported ∼48 hours) or contrastive baselines that require large batch sizes for convergence.

Inference Throughput and Scalability. We benchmark system efficiency on the Spectraverse test set.

- **Online Query Latency:** $\approx$ 100 ms to encode a spectrum, followed by $<$ 0.1 ms for retrieval against a pre-computed FAISS index.
- **Offline Indexing Speed:** The frozen molecular encoder enables rapid database construction, processing $\approx$ **4,900 molecules per second** (0.20 ms/mol) on a standard GPU.

This high throughput ($\approx$ 250 queries per second batched) makes SpecBridge suitable for real-time metabolomics workflows and allows for frequent updates to large-scale reference libraries. In contrast, autoregressive generative models typically process $<$ 10 queries per second.

A.7. Quantitative Candidate Hardness Analysis

To quantify the intrinsic difficulty of the retrieval tasks, we computed the Tanimoto similarity (Morgan fingerprints, radius 2, 4096 bits) between the ground truth molecule and every candidate in its pool. We define "hardness" as the maximum similarity found among the decoys.

Results. Table 9 and Figure 5 summarize the results.

- **MassSpecGym (Scaffold Retrieval):** The candidate pools rarely contain close analogues. The mean maximum similarity is 0.55, and only 1.4 candidates per pool exceed a similarity threshold of 0.8.
- **Spectraverse (Isomer Resolution):** The PubChem-derived pools are significantly denser with structurally similar decoys. The mean maximum similarity is 0.69, with an average of 11.9 candidates per pool exceeding 0.8 similarity.

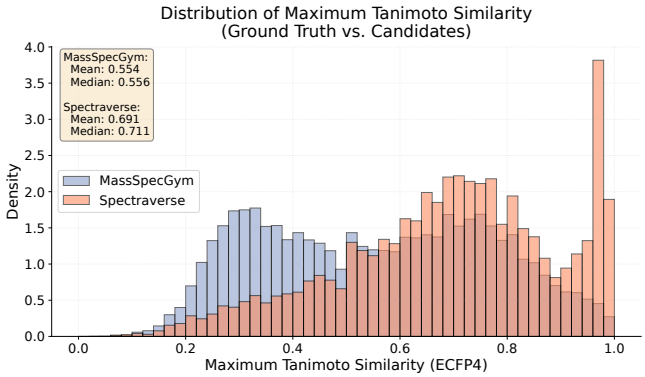

Figure 5. **Distribution of Maximum Candidate Similarity.** Histograms of the maximum Tanimoto similarity between the ground truth and the hardest decoy.

Table 9. **Intrinsic Difficulty Statistics.** Comparison of candidate pools.

Metric	**MassSpecGym**	**Spectraverse**
Mean Max Similarity	0.55	**0.69**
Median Max Similarity	0.56	**0.71**
Hard Candidates ($>$ 0.8)	1.4	**11.9**